Pis'ma v ZhETF, vol. 89, iss. 3, pp. 127 – 132

Manifestly-covariant p^3 calculation of nucleon Compton scattering

V. Lensky[1) +*], *V. Pascalutsa*[+∇]

[+]*European Centre for Theoretical Studies in Nuclear Physics and Related Areas (ECT*), Villazzano (Trento), I-38050 TN, Italy*

[*]*Institute for Theoretical and Experimental Physics, 117218 Moscow, Russia*

[∇]*Institut für Kernphysik, Johannes Gutenberg Universität, Mainz D-55099, Germany*

Submitted 5 November 2008

We compute the Compton scattering off the nucleons in the framework of manifestly covariant baryon chiral perturbation theory (BχPT). The results for observables differ substantially from the corresponding calculations in heavy-baryon chiral perturbation theory (HBχPT), most appreciably in the forward kinematics. We verify that the covariant p^3 result fulfills the forward-Compton-scattering sum rules. We also explore the effect of the $\Delta(1232)$ resonance at order p^4/Δ, with $\Delta \approx 300\,$MeV, the resonance excitation energy. We find that the substantial effect of the Δ-excitation on the nucleon polarizabilities can naturally be accommodated in the manifestly covariant calculation.

PACS: 13.60.Fz, 14.20.Dh, 25.20.Dc

1. Introduction. Compton scattering off nucleons is a unique tool to study the structure and the e.m. properties of the nucleon. The e.m. properties are probed already at very low energies (soft photons), where the process depends on the static e.m. moments of the target, the charge and magnetic moment in the case of the nucleon [1]. To probe the structure, the energy of the incident photons must be sufficiently high, their wavelength to be comparable with the nucleon size.

From a pedestrian point of view the nucleon consists of a quark core surrounded by a cloud of pions. The quark core is confined to a radius of less than a fermi, while the pion cloud can extend to as much as 1.5 fm. And indeed, at energies of around 100 MeV and above, the effects of the nucleon structure become significant enough to be detected in modern Compton-scattering experiments [2 – 6] (see Refs. [7, 8] for review). More specifically, it has been possible to detect the nucleon *polarizabilities*, with the result shown in the PDG column of the Table. These values clearly point out the composite structure of the nucleon (for a classical pointlike object polarizabilities vanish). More insights come from studying these quantities in chiral perturbation theory (χPT), an effective theory of the low-energy strong interaction [9, 10].

In χPT, the leading-order result for the nucleon polarizabilities is a prediction, in the sense that the low-energy constants (LECs) associated with polarizabilities do not enter until the next order. The whole result is given by a few chiral loops, quantified in terms of well-known parameters, such the nucleon and pion masses (M_N and m_π) and the pion-nucleon coupling constant, $g_{\pi NN}$. The first calculation of polarizabilities in χPT, carried out by Bernard, Kaiser and Meißner [11], at leading order yields the values shown in the BχPT $\mathcal{O}(p^3)$ column of the Table.

This first calculation has been carried out in what now is called *manifestly Lorentz-covariant* baryon chiral perturbation theory (BχPT), to distinguish it from the heavy-baryon chiral perturbation theory (HBχPT). The heavy-baryon formalism was carried over from the heavy-quark QCD to χPT [15] in order to cure the problems with chiral power counting, which BχPT had apparently had [16]. Incidentally, the HBχPT result (which is easily obtained from [11] by keeping only the leading in m_π/M_N term) happens to agree with experiment much better, see the Table. Subsequently, more sophisticated analyses of Compton scattering in HBχPT followed [12, 17, 18], while the original result [11] received less attention.

More recently, however, Gegelia *et al.* [19, 20] realized that BχPT does not have a problem with power counting *per se*. The pieces that were thought to violate the power counting are compensated (renormalized) by the available LECs and therefore do not alter the physics. At the same time, Becher and Leutwyler [21] pointed out that the difference between BχPT and HBχPT result can be unnaturally large due to the presence of physical cuts and other non-analytic structures which do not easily admit a polynomial expansion. Also, it

[1)] e-mail: lensky@ect.it

The electric (α) and magnetic (β) polarizabilities of the proton in units of $10^{-4}\,\mathrm{fm}^3$. The last column quotes the Particle Data Group compilation of experimental results, while the first two represent the predictions of the heavy-baryon and manifestly-covariant χPT, respectively

	HBχPT		BχPT		PDG
	$\mathcal{O}(p^3)$ [12]	$\mathcal{O}(\epsilon^3)$ [13]	$\mathcal{O}(p^3)$ [11]*	$\mathcal{O}(p^4/\Delta)$	[14]
$\alpha^{(p)}$	12.2	20.8	6.8	10.8	12.0 ± 0.6
$\beta^{(p)}$	1.22	14.7	-1.8	2.9	1.9 ± 0.5

*The values differ from the ones quoted in Ref. [11] because of the value of the πNN coupling constant: $g_{\pi NN} = 13.4$ in [11] versus $g_{\pi NN} = g_A M_N / f_\pi \simeq 12.9$ in this work and in [12].

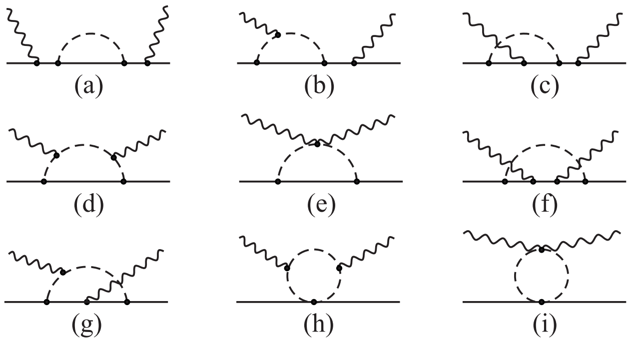

Fig.1. The loop graphs evaluated in this work. Graphs obtained from these by crossing and time-reversal are not shown, but are evaluated too

has been noted that HBχPT is incompatible with the dispersion relations and sum rules [22–24]. Finally, the effect of the Δ excitation in Compton scattering cannot be accommodated in the HB framework in any natural way [25, 26] (see also the HBχPT column of the Table). All these observations make a strong case for adopting the manifestly-covariant formalism in favor of the heavy-baryon one. The present work is the first step towards this goal.

In this letter we present the calculation of Compton scattering in BχPT, to orders p^3 and p^4/Δ. In Sect. 2 we consider the graphs needed to be computed and explain how we compute them. In Sect. 3, we verify that the BχPT result is consistent with the Compton-scattering sum rules. We also elaborate on the impact that chiral symmetry makes on nucleon polarizabilities. In Sect. 4 we show the results for the Compton scattering cross-sections. We conclude with Sect. 5.

2. Chiral loops and Lagrangians. The chiral power counting for the Compton amplitude in χPT with pions and nucleons is reviewed in [11, 12]. Reference [11] also shows the one-loop graphs that arise at $\mathcal{O}(p^3)$, even if it only considers the contribution of those graphs to the scalar polarizabilities.

The chiral expansion for the Compton amplitude begins at order p^2, where it receives contributions from the Born graphs only. At $\mathcal{O}(p^3)$ there are contributions from a number of loop graphs displayed in Fig.1 and the Wess-Zumino-Witten (WZW) anomaly graph. The expression for the Born and WZW-anomaly contributions can be found in, e.g., [26], while here we focus on the loop graphs.

Note that the graphs in Fig.1 are not exactly the same as found in [11], however they will lead to exactly the same result. This is because we use a different, albeit *equivalent*, in the sense of 'equivalence theorem', form of the Lagrangian. To explain that, let us consider the leading-order chiral Lagrangian for the nucleon:

$$\mathcal{L}_N^{(1)} = \overline{N}\,(i\rlap{/}D - M_N + g_A\,\rlap{/}a\,\gamma_5)\,N, \qquad (1)$$

where N denotes the isodoublet Dirac field of the nucleon, M_N is the nucleon mass and g_A is the axial-coupling constant, both taken at their chiral-limit value. Furthermore, the chiral covariant derivative is given by

$$D_\mu N = \partial_\mu N + i v_\mu N, \qquad (2)$$

whereas the vector and axial-vector fields above are defined in terms of the pion field, $\pi^a(x)$, as

$$v_\mu \equiv \frac{1}{2}\,\tau^a v_\mu^a(x) = \frac{1}{2i}\left(u\,\partial_\mu u^\dagger + u^\dagger \partial_\mu u\right), \qquad (3a)$$

$$a_\mu \equiv \frac{1}{2}\,\tau^a a_\mu^a(x) = \frac{1}{2i}\left(u^\dagger\,\partial_\mu u - u\,\partial_\mu u^\dagger\right), \qquad (3b)$$

with $u = \exp(i\pi^a\tau^a/2f)$, an $SU(2)$ matrix, and f the pion decay constant in the chiral limit.

Let us now consider a redefinition of the nucleon field, $N \to \xi N$, where the field ξ has the following form:

$$\xi = \exp\left(\frac{i g_A\,\pi^a\tau^a}{2f}\gamma_5\right). \qquad (4)$$

Our first-order chiral Lagrangian then becomes:[2)]

$$\begin{aligned} \mathcal{L'}_N^{(1)} &= \overline{N}\,\xi\,(i\rlap{/}D - M_N + g_A\,\rlap{/}a\,\gamma_5)\,\xi\,N = \\ &= \overline{N}\,(i\rlap{/}\partial - M_N)\,N + M_N\,\overline{N}\,(1-\xi^2)N + \\ &\quad + \overline{N}\,(\xi\,i\rlap{/}\partial\xi - \xi\,\rlap{/}v\,\xi + g_A\,\xi\,\rlap{/}a\,\gamma_5\,\xi)\,N. \end{aligned} \qquad (5)$$

Both Lagrangians, Eq. (1) and Eq. (5), are equivalent, however, may have drastically different forms when

[2)] In our conventions $\gamma_5^\dagger = \gamma_5$, hence $\xi^\dagger = \exp(-ig\pi^a\tau^a\gamma_5/2f_\pi)$, $\xi\xi^\dagger = 1$. Note also that $\overline{N} \to \overline{N}\xi$, and $\xi\gamma^\mu\xi = \gamma^\mu$.

expanded in the pion field. For the one-loop contributions to Compton scattering it is sufficient to expand up to the second order in the pion field:

$$v_\mu = \frac{1}{4f^2}\,\tau^a \varepsilon^{abc}\pi^b\,\partial_\mu \pi^c + O(\pi^3), \tag{6a}$$

$$a_\mu = \frac{1}{2f}\tau^a \partial_\mu \pi^a + O(\pi^3), \tag{6b}$$

$$\xi = 1 + \frac{ig_A}{2f}\tau^a\pi^a\gamma_5 - \frac{g_A^2}{8f^2}\pi^2 + O(\pi^3). \tag{6c}$$

The original and the redefined Lagrangians take, respectively, the following form:

$$\mathcal{L}_N^{(1)} = \overline{N}\left(i\partial\!\!\!/ - M_N + \frac{g_A}{2f}\tau^a \partial\!\!\!/\pi^a\gamma_5 - \right.$$
$$\left. - \frac{1}{4f^2}\,\tau^a\varepsilon^{abc}\pi^b\,\partial\!\!\!/\pi^c\right) N + O(\pi^3), \tag{7}$$

$$\mathcal{L}'^{(1)}_N = \overline{N}\left(i\partial\!\!\!/ - M_N - i\,\frac{g_A}{f}M_N\tau^a\pi^a\gamma_5 + \right.$$
$$\left. + \frac{g_A^2}{2f^2}M_N\pi^2 - \frac{(g_A-1)^2}{4f^2}\tau^a\varepsilon^{abc}\pi^b\,\partial\!\!\!/\pi^c\right) N + O(\pi^3). \tag{8}$$

The major difference between the two forms is that the pseudovector πNN coupling is transformed into a pseudoscalar one, while the Weinberg-Tomozawa $\pi\pi NN$ term is replaced by an isoscalar term akin to the remains of an integrated-out σ-meson in the linear sigma model. The new isovector $\pi\pi NN$ term, proportional to $(g_A-1)^2$ does not give any contribution to Compton amplitude at one-loop level.

Also, at the order that loops are considered, the photon couples only minimally, i.e., to the electric charge of the pion and nucleon.[3)] Now that the pion couples to the nucleon via pseudoscalar coupling, there is no Kroll-Ruderman ($\gamma\pi NN$) term arising, and hence the number of one-loop graphs is severely reduced.

Thus, the loop graphs shown in [11] with couplings from the Lagrangian (7) transform to the graphs shown in Fig.1 with the couplings from (8). We have checked explicitly that the two sets of one-loop diagrams give identical expressions for the Compton amplitude.

The purpose of the above field-redefinition 'trick' is to simplify the calculation, but it also explains why Metz and Drechsel [27], calculating polarizabilities in the linear sigma model with heavy σ-meson, obtain to one loop exactly the same result as BχPT at $\mathcal{O}(p^3)$ [11]. Indeed, we can see that the two calculations are related through a field redefinition and therefore bound to give the same results for physical quantities.

[3)]Not in the Born graphs, where the anomalous magnetic moment of the nucleon appears too at this order.

A word on renormalization. The one-particle-reducible graphs in Figs.1 and 2 contribute to the nucleon mass, field, charge, and magnetic moment renormalization. We have adopted the on-mass-shell renormalization scheme, and used then the following values of the parameters: $e^2/4\pi = 1/137$, $g_A = 1.267$, $f = f_\pi = 0.0924$ GeV, $m_\pi = 0.139$ GeV, $M_N = 0.9383$ GeV, $\kappa_N = 1.79$ for the proton.

The Δ contribution is included here within the framework developed in Ref. [26]. A study of the Δ-resonance contributions is necessary before embarking on to the p^4 calculations, since some of the Δ-contributions are of order p^4/Δ, where $\Delta = M_\Delta - M_N \approx 0.3$ GeV. The diagrams that contribute at that order are shown in Fig.2. The first graph, the Δ Born contribu-

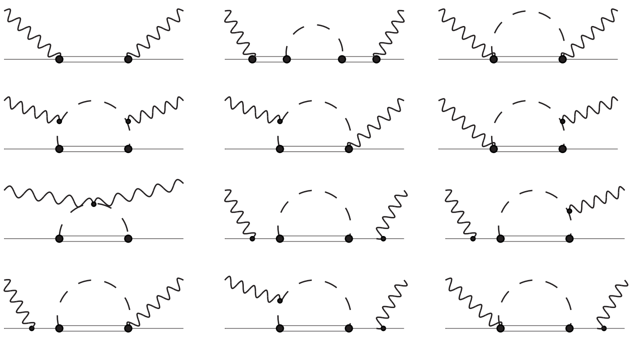

Fig.2. The graphs with $\Delta(1232)$ that contribute at order p^4/Δ. Graphs obtained from these by crossing are not shown, but are calculated as well

tion has been calculated in the same way as in Ref. [26], except that now we have used the values of the $\gamma N \to \Delta$ transition parameters ($g_M = 2.95$ and $g_E = -1.0$) from the pion-photoproduction analyses of Refs. [32, 33], and also included the corresponding crossed graph. For the $\pi N\Delta$ coupling we have used $h_A = 2.85$, the value inferred from the $\Delta \to \pi N$ decay width of 115 MeV.

The loop graphs in Figs.1 and 2 were eventually computed by us with the help of algebraic tool FORM [28] and the LoopTools library [29]. More details will be given in a subsequent publication. In the rest of this letter we deal with the results of these calculations.

3. Consistency with sum rules. The dispersion relations enjoy a special role in nucleon Compton scattering, see Ref. [7] for a nice review. To begin with, practically all empirical values of nucleon polarizabilities are extracted from data with the use of a model based on dispersion relations [30, 31]. Furthermore, in the forward kinematics, the Compton amplitude can be related to an integral over energy of the photoabsorption cross-section, which in combination with the low-energy expansion yields a number of model-independent sum rules. A famous example is the Baldin sum rule:

$$\alpha+\beta = \frac{1}{2\pi^2}\int_0^\infty d\omega \frac{\sigma_T(\omega)}{\omega^2 - i0}, \tag{9}$$

where the sum of polarizabilities is related to an integral of the total photoabsorption cross-section σ_T.

In general, the forward Compton-scattering amplitude can be decomposed into two scalar functions of single variable in the following way:

$$T_{fi}(\omega) = \boldsymbol{\epsilon}'^* \cdot \boldsymbol{\epsilon}\, f(\omega) + i\boldsymbol{\sigma}\cdot(\boldsymbol{\epsilon}'^* \times \boldsymbol{\epsilon})\,\omega\, g(\omega), \tag{10}$$

where $\boldsymbol{\epsilon}'$, $\boldsymbol{\epsilon}$ are the polarization vectors of the initial and final photons, respectively, and $\boldsymbol{\sigma}$ are the Pauli spin matrices. The functions f and g are even functions of the photon energy ω. Using analyticity and the optical theorem (unitarity) one can write down the following sum rules:

$$f(\omega) = f(0) + \frac{\omega^2}{2\pi^2}\int_0^\infty d\omega' \frac{\sigma_T(\omega')}{\omega'^2 - \omega^2 - i0}, \tag{11a}$$

$$g(\omega) = \frac{1}{4\pi^2}\int_0^\infty d\omega'\,\omega'\,\frac{\sigma_{1/2}(\omega') - \sigma_{3/2}(\omega')}{\omega'^2 - \omega^2 - i0}, \tag{11b}$$

where σ_λ is the doubly-polarized photoabsorption cross-section, with λ being the helicity of the initial photon-nucleon state.

These sum rules should also hold for the individual contributions of the loop graphs in Fig.1. In this case the photoabsorption process is given by the leading-order single-pion photoproduction, for which analytic expressions exist [24]. We were able to verify that the (renormalized) p^3 loop contributions in Fig.1 fulfill the sum rules (11) exactly.

It is interesting to note that the leading-order pion photoproduction amplitude, which enters on the right-hand side of (11), is independent of whether one uses pseudovector or pseudoscalar πNN coupling. It essentially means that chiral symmetry is not relevant at this order. The latter statement can, by means of the sum rule, be extended to the forward Compton amplitude at $\mathcal{O}(p^3)$. On the other hand, the graphs (h) and (i) in Fig.1, being the only ones beyond the pseudoscalar theory, take the sole role of chiral symmetry. In the forward kinematics these graphs indeed vanish, but play an important role in the backward angles. Without them the values of α and β would be entirely different. The value of $\alpha+\beta$ would of course be the same, but $\alpha-\beta$ would (approximately) flip the sign. Furthermore, in the chiral limit, the value of $\alpha-\beta$ would diverge as $1/m_\pi^2$ (instead of $1/m_\pi$ as it should). In this way we arrive at the conclusion that chiral symmetry plays a more prominent role in the backward Compton scattering.

The resulting values for the polarizabilities, however, are in worse agreement with experiment than the HBχPT p^3 result (see the Table). This, in fact, is a big success of the covariant calculation – it opens a room for the $\Delta(1232)$-resonance contributions. The Δ-excitation plays an important role in nucleon polarizabilities, as can already be seen from the Baldin sum rule and the fact that the photoabsorption cross-section is dominated, at lower energies, by the Δ resonance. In BχPT we will see the Δ playing the same prominent role on both sides of the sum rule. In contrast, the HBχPT p^3 value for $\alpha+\beta$ already saturates the sum rule, leaving no room for other contributions.

4. Results for observables. First let us see how the differences between the HBχPT and BχPT show up in observables. In Fig.3, we consider the unpolarized differential cross-section of the $\gamma p \to \gamma p$ process as a

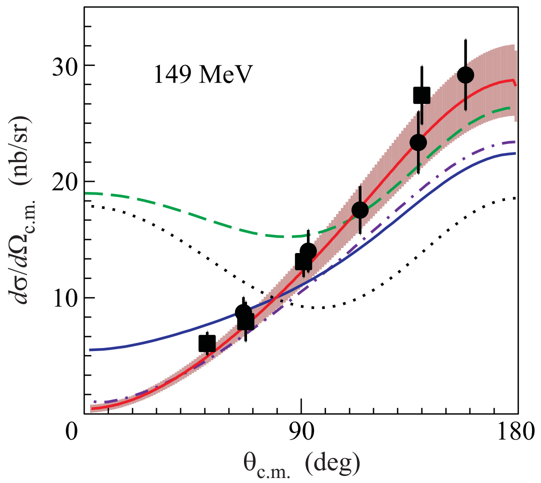

Fig.3. (Color online) Angular dependence of the $\gamma p \to \gamma p$ differential cross-section in the center-of-mass system for fixed photon-beam energy, $E_\gamma^{(lab)} = 149$ MeV. Data points are from SAL [4] – filled squares, and MAMI [6] – filled circles. The curves are: Klein-Nishina – dotted, Born graphs and WZW-anomaly – green dashed, adding the HBχPT – violet dash-dotted, adding the BχPT – blue solid. The result of adding the Δ-excitation contribution to the BχPT p^3 is shown by the red solid line with a band

function of the scattering angle in center-of-mass system, with the incident photon energy fixed at just below the pion-production threshold. The dotted line represents the Klein-Nishina cross-section (scattering off a classical pointlike 'proton'). The dashed line adds on the anomalous magnetic moment and the π^0 anomaly contributions. Then the effect of the p^3 HBχPT result is indicated by the dash-dotted line, in contrast to the effect BχPT result which is given by the blue solid line.

Clearly, the major differences between the two p^3 calculations arise at forward angles. This is because at low energies the p^3 contribution to the cross-section at forward (and backward) angles is determined by the p^3 contribution to $\alpha+\beta$ (and $\alpha-\beta$). We have seen already from the Table that the sum of polarizabilities differs between the two calculations much more than their difference, and this fact reflects itself in the cross-section.

The red solid line with an error band in Fig.3 shows the result of adding the $\Delta(1232)$-resonance contribution to the covariant p^3 result. The fact that the Δ contribution in BχPT is compatible with both photoproduction and Compton scattering data is further demonstrated in Fig.4, where the Compton scattering cross-section is plotted as a function of photon energies at fixed angles (in the lab system). The legend for the curves is the same as in the previous figure. The HBχPT result is omitted here, but can be found in Ref. [18]. The results for the nucleon proton polarizabilities, complete up to $\mathcal{O}(p^4/\Delta)$, are displayed in the corresponding column of the Table.

We emphasize that, while the fit in [26], where the HBχPT p^3 result was used, demanded a re-adjustment of the $\gamma N\Delta$ parameters to unrealistic values, the present BχPT result allows for the correct values of the $\gamma N\Delta$ parameters. Therefore up to the order p^4/Δ there are no fitting parameters. This is a prediction of BχPT.

5. Conclusion. We have studied the nucleon Compton scattering in the framework of BχPT at orders p^3 and p^4/Δ. These are 'predictive' calculations in the sense that there are no new low-energy constants, they come starting at order p^4. We find that the covariant p^3 result fulfills the forward-Compton-scattering sum rules, while the HBχPT result does not. Chiral symmetry has no effect on the forward Compton scattering but plays an important role at the backward scattering. Examining the Compton-scattering cross sections we find that the difference between the HBχPT and BχPT results can indeed be unnaturally large, most notably in the forward kinematics. We argue that higher-order effects of the $\Delta(1232)$-resonance excitation can more naturally be accommodated in the manifestly covariant calculation. This is due to partial cancellation of the relativistic and Δ-excitation effects which is explicit in the covariant calculation. In contrast to the HBχPT approach, in BχPT the effect of $\Delta(1232)$ appears to be compatible both with the Compton scattering and pion photoproduction data.

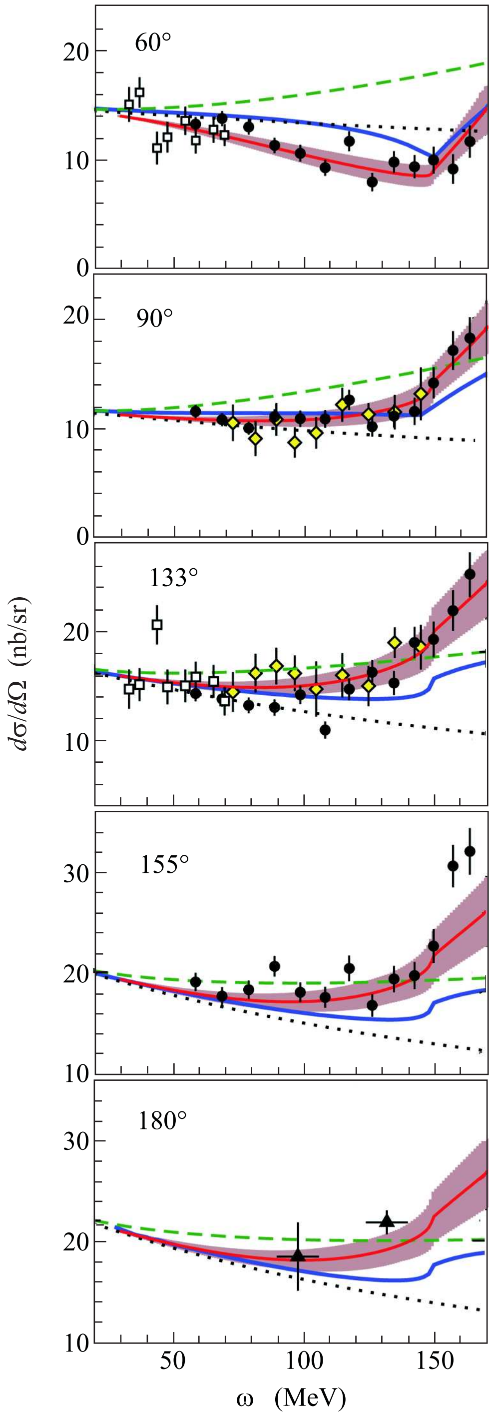

Fig.4. (Color online) Energy-dependence of the $\gamma p \to \gamma p$ differential cross-section in the laboratory frame for fixed values of the scattering angle. Data points are from: Illinois [2] – open squares, MAMI [3] – filled triangles, SAL [5] – open diamonds, and MAMI [6] – filled circles. The legend for the curves is the same as in Fig.3

We thank J. Gegelia and M. Vanderhaeghen for reading the manuscript and useful remarks. This work is partially supported by the European Community Research Infrastructure Activity under the FP6 "Structuring the

European Research Area" programme (HadronPhysics, contract # RII3-CT-2004-506078).

1. F. E. Low, Phys. Rev. **96**, 1428 (1954); M. Gell-Mann and M. L. Goldberger, Phys. Rev. **96**, 1433 (1954).
2. F. J. Federspiel et al., Phys. Rev. Lett. **67**, 1511 (1991).
3. A. Zieger, R. Van de Vyver, D. Christmann et al., Phys. Lett. B **278**, 34 (1992).
4. E. L. Hallin et al., Phys. Rev. C **48**, 1497 (1993).
5. B. E. MacGibbon, G. Garino, M. A. Lucas et al., Phys. Rev. C **52**, 2097 (1995).
6. V. Olmos de Leon et al., Eur. Phys. J. A **10**, 207 (2001).
7. D. Drechsel, B. Pasquini, and M. Vanderhaeghen, Phys. Rept. **378**, 99 (2003).
8. M. Schumacher, Prog. Part. Nucl. Phys. **55**, 567 (2005).
9. S. Weinberg, Physica A **96**, 327 (1979).
10. J. Gasser and H. Leutwyler, Ann. Phys. **158**, 142 (1984); Nucl. Phys. B **250**, 465 (1985).
11. V. Bernard, N. Kaiser, and U.-G. Meißner, Phys. Rev. Lett. **67**, 1515 (1991); Nucl. Phys. B **373**, 346 (1992).
12. V. Bernard, N. Kaiser, and U.-G. Meißner, Int. J. Mod. Phys. E **4**, 193 (1995).
13. T. R. Hemmert, B. R. Holstein, and J. Kambor, Phys. Rev. D **55**, 5598 (1997).
14. W. M. Yao et al. [Particle Data Group], J. Phys. G **33**, 1 (2006).
15. E. Jenkins and A. V. Manohar, Phys. Lett. B **255**, 558 (1991).
16. J. Gasser, M. E. Sainio, and A. Svarc, Nucl. Phys. B **307**, 779 (1988).
17. J. A. McGovern, Phys. Rev. C **63**, 064608 (2001) [Erratum-ibid. C **66**, 039902 (2002)].
18. S. R. Beane, M. Malheiro, J. A. McGovern et al., Phys. Lett. B **567**, 200 (2003) [Erratum-ibid. B **607**, 320 (2005)]; Nucl. Phys. A **747**, 311 (2005).
19. J. Gegelia and G. Japaridze, Phys. Rev. D **60**, 114038 (1999); J. Gegelia, G. Japaridze, and X. Q. Wang, J. Phys. G **29**, 2303 (2003).
20. T. Fuchs, J. Gegelia, G. Japaridze, and S. Scherer, Phys. Rev. D **68**, 056005 (2003).
21. T. Becher and H. Leutwyler, Eur. Phys. J. C **9**, 643 (1999).
22. A. I. L'vov, Phys. Lett. B **304**, 29 (1993).
23. V. Pascalutsa, B. R. Holstein, and M. Vanderhaeghen, Phys. Lett. B **600**, 239 (2004).
24. B. R. Holstein, V. Pascalutsa, and M. Vanderhaeghen, Phys. Rev. D **72**, 094014 (2005).
25. R. P. Hildebrandt, H. W. Griesshammer, T. R. Hemmert, and B. Pasquini, Eur. Phys. J. A **20**, 293 (2004).
26. V. Pascalutsa and D. R. Phillips, Phys. Rev. C **67**, 055202 (2003).
27. A. Metz and D. Drechsel, Z. Phys. A **356**, 351 (1996).
28. J. Vermaseren, *Symbolic Manipulation with FORM*, Computer Algebra Nederland, Amsterdam, 1991.
29. T. Hahn and M. Rauch, Nucl. Phys. Proc. Suppl. **157**, 236 (2006).
30. A. I. L'vov, Sov. J. Nucl. Phys. **34**, 597 (1981) [Yad. Fiz. **34**, 1075 (1981)].
31. A. I. L'vov, V. A. Petrun'kin, and M. Schumacher, Phys. Rev. C **55**, 359 (1997).
32. V. Pascalutsa and M. Vanderhaeghen, Phys. Rev. Lett. **95**, 232001 (2005); Phys. Rev. D **73**, 034003 (2006).
33. V. Pascalutsa, M. Vanderhaeghen, and S. N. Yang, Phys. Rept. **437**, 125 (2007).